

Probing light bino and higgsinos at the LHC

Chengcheng Han

*Asia Pacific Center for Theoretical Physics,
San 31, Hyoja-dong, Nam-gu,
Pohang 790-784, Republic of Korea*

Abstract

Motivated by the naturalness, we study a simplified MSSM scenario where only the bino-like LSP and higgsino-like NLSP are light. We first scan the parameter space of this scenario, considering the constraints from the Higgs mass, flavor physics, electroweak precision measurements and dark matter experiments. Then in the allowed parameter space, we perform a Monte Carlo simulation for the $\tilde{\chi}_1^\pm \tilde{\chi}_{2,3}^0$ production followed by $\tilde{\chi}_1^\pm \rightarrow W^\pm \tilde{\chi}_1^0$ and $\tilde{\chi}_{2,3}^0 \rightarrow Z \tilde{\chi}_1^0$. By examining the presently available trilepton bounds on the wino-like chargino/neutralino, we find that only a narrow region $40 \text{ GeV} \lesssim m_{\tilde{\chi}_1^0} \lesssim 50 \text{ GeV}$ and $160 \text{ GeV} \lesssim m_{\tilde{\chi}_{2,3}^0} \lesssim 170 \text{ GeV}$ on the plane of $m_{\tilde{\chi}_1^0} - m_{\tilde{\chi}_{2,3}^0}$ can be excluded. Finally, we explore the potential of trilepton signature in probing such a scenario at 14 TeV LHC and find that the region with $40 \text{ GeV} \lesssim m_{\tilde{\chi}_1^0} \lesssim 60 \text{ GeV}$ and $160 \text{ GeV} \lesssim m_{\tilde{\chi}_{2,3}^0} \lesssim 300 \text{ GeV}$ can be covered at 3σ level with luminosity $\mathcal{L} = 300 \text{ fb}^{-1}$.

PACS numbers:

I. INTRODUCTION

The ATLAS and CMS have observed the Higgs boson [1] and up to now the measurements of Higgs properties consist with the standard model (SM) predictions. However, the SM suffers from the so-called naturalness problem [2] which inspires theorists to propose various new physics models. Among these new physics models the natural SUSY [3–7] satisfied the naturalness criterion perfectly. It needs a light stop sector and a weak scale higgsino mass $\mu \lesssim O(300 \text{ GeV})$. The stop sector in the natural SUSY has been discussed extensively [8–11]. The weak scale higgsino in the natural SUSY results in the existence of at least two light neutralinos and a pair of charginos at the weak scale. If the lighter one of the two neutralinos is the dark matter, the dark matter relic density would be far below the observed one because a higgsino like dark matter usually has large annihilation cross section to the SM particles. However if the bino is the LSP, then the dark matter is bino like and has some higgsino component, the dark matter relic density could much easier to be satisfied. So searching for such kinds of electroweakinos would directly probe the dark matter sector and the naturalness of SUSY.

Generally, the search strategies depends on the spectrum of electroweakinos. If the electroweakinos are highly degenerate at low energy, they could be probed by the mono-jet, mono-photon or mono- Z in the future experiments [12–14]. One such case is, at weak scale, only the higgsinos are light. In this case, the mono-jet signal can search higgsinos to 150 GeV at 2σ level at 14TeV LHC with luminosity 3000 fb^{-1} .

If the mass splitting between the electroweakinos is moderate, they can be probed through multi-soft leptons [15]. Recently, some authors also proposed a new channel $\ell^+\ell^- + \gamma + \cancel{E}_T$ to probe the region with a small splitting between the higgsinos and bino [16]. The photon in the final state comes from the χ_2^0 decaying into χ_1^0 plus a photon, and the two leptons come from the other neutralino decaying into LSP via a virtual Z boson. When the splitting between the two neutralinos is small, the branching ratio of $\chi_2^0 \rightarrow \gamma\chi_1^0$ is considerable. So, another signal $j + \ell + \gamma + \cancel{E}_T$ from neutralino/chargino pair production may be also accessible at the future LHC [17].

If the electroweakinos have a large mass splitting, the multi-leptons final state from chargino/neutralino pair production has the highest sensitivity [18, 19]. The ATLAS and CMS collaborations performed such a study and gave the mass limits $m_{\tilde{\chi}_1^\pm, \tilde{\chi}_2^0} > 345 \text{ GeV}$

(ATLAS) [20] and $m_{\tilde{\chi}_1^\pm, \tilde{\chi}_2^0} > 270$ GeV (CMS) [21] assuming the chargino/neutralino decays via intermediate gauge bosons and the LSP is almost massless. But this limit depends on the component of chargino/neutralino. In the experiment, a wino NLSP and bino LSP are assumed and thus the pair produced chargino/neutralino are wino-like. The limit would be changed if the NLSP is higgsino. One reason is that the cross section of chargino/neutralino production in the wino NLSP case is larger than the one in the higgsino case. The other reason is that in the realistic spectrum, the decay branching ratio of $\chi_2^0 \rightarrow \chi_1^0 + Z$ is not 100% since χ_2^0 could decay into $\chi_1^0 + h$.

In the present work, we focus on the LSP bino and NLSP higgsino case. We also require the wino decoupled. Such kinds of spectrums can be realized in the non-universal gaugino masses models. We reinterpreted the experiments results in the realistic spectrum, and give the prospect of detecting this signal in the future LHC experiments.

The rest of this paper is organized as follows: In Sec. II, we scan the parameter space, and the properties of the surviving parameter space are investigated. In Sec. III, we reinterpret the experimental limits on the parameter space. In Sec. IV, the prospect of detecting this signal in our surviving space are studied.

II. THE PROPERTY OF SURVIVING PARAMETER SPACE

In this section, we scan the parameter space in the frame of natural SUSY with a light bino. Some survived samples are shown, which are susceptible to the $3l$ experiment and possible closed by future direct search results.

The parameter space are scanned in the following region:

$$1 \text{ GeV} < M_1 < 100 \text{ GeV}, \quad 100 \text{ GeV} < \mu < 300 \text{ GeV}, \quad 3 < \tan \beta < 60, \quad (1)$$

where the lower bound of μ avoids the chargino search limit and upper bound satisfies the naturalness requirement. Other parameters, except for the stop sector, are fix at 2 TeV. The stop sector are scanned in this region,

$$700 \text{ GeV} < (M_{\tilde{Q}_3}, M_{\tilde{t}_R}) < 2 \text{ TeV}, \quad -3 \text{ TeV} < A_t < 3 \text{ TeV} \quad (2)$$

where the lower bound avoids the direct stop search limit and the upper bound keeps the naturalness of the SUSY.

The following constraints are considered in the scan:

- (1) The SM-like Higgs mass is required to within the range of 123–127 GeV. We use **FeynHiggs2.8.9** [22] to calculate the Higgs mass, and impose the experimental constraints from LEP, Tevatron and LHC by **HiggsBounds-3.8.0** [23].
- (2) We require our samples to satisfy various B-physics bounds at 2σ level. We use **SuperIso v3.3** [24] to implement the constraints, including $B \rightarrow X_s \gamma$ and the latest measurements of $B_s \rightarrow \mu^+ \mu^-$, $B_d \rightarrow X_s \mu^+ \mu^-$ and $B^+ \rightarrow \tau^+ \nu$.
- (3) The SUSY prediction of the precision electroweak observable, such as ρ_t , $\sin^2 \theta_{\text{eff}}^l$, m_W and R_b [25], are required to be within the 2σ ranges of the experimental values.
- (4) A light bino in the natural SUSY would mix with the higgsino, which induces three neutralinos and a pair of charginos. The lightest neutralino acts as the dark matter candidate. So the relic abundance and the direct search of the dark matter set limit on the parameter space. Here we require the thermal relic density of the lightest neutralino (as the dark matter candidate) is under the 2σ upper limit of the Planck value [26]. We use the code **MicrOmega v2.4** [27] to calculate the relic abundance and DM-nucleon scattering.

Figure 1 shows the dark matter properties in the surviving space. The left panel scatters the relic abundance of the surviving samples. We can see that there are two regions left both of which have a bino like dark matter, requiring the 2σ upper limit of the Planck value [26]. The first region corresponding a lighter dark matter mass lying in $35 \sim 50$ GeV near half of the Z boson mass. In the other region, the dark matter mass lies in $50 - 65$ GeV near half of the Higgs mass. It is easy to explain it. Usually, a bino LSP has a small annihilation cross section and thus it is easy to get a large relic density. If there is a particle in the s-channel, the annihilation cross section can be raised through resonance enhancement and thus the relic abundance are reduced. It requires that the dark matter mass is around half of the boson mass. In our spectrum, only the Z boson or the Higgs boson can play this role. We should note there are points satisfying the 2σ range of PLANCK. These points could get the correct relic abundance due to joint effect of the resonance and the mixing between bino and higgsino [28].

The right panel shows the limit of dark matter direct search. It tells that the Z/h resonance region easily get rid of the LUX [29] constraint, due to the moderate spitting

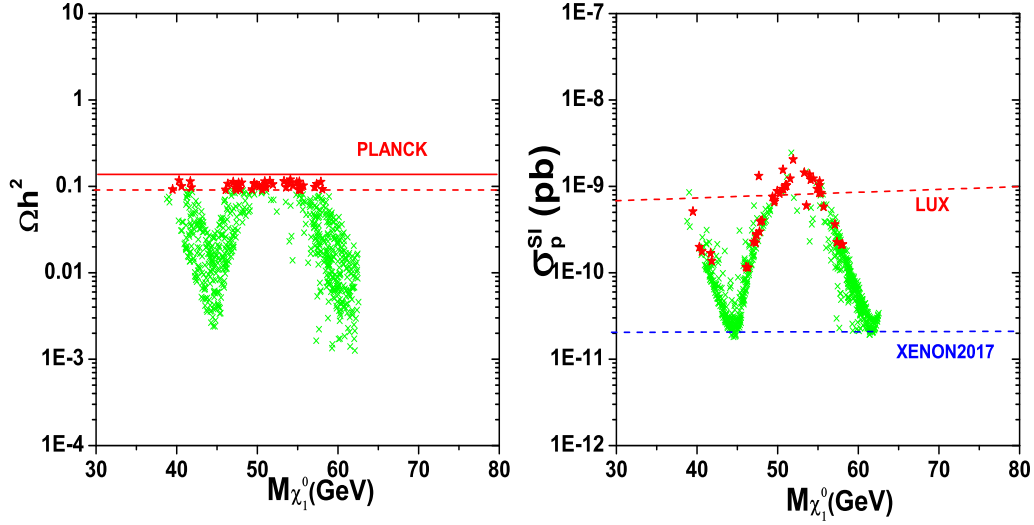


FIG. 1: Dark matter properties in the surviving space. All points satisfy 2σ upper limit of PLANCK. The red pentagrams locate within the 2σ range of PLANCK, $0.091 < \Omega h^2 < 0.138$, where a 10% theoretical uncertainty is included. The DM-nucleon scattering cross section has been scaled by a factor $\Omega h^2 / \Omega h^2(PLANCK)$.

between bino and higgsino. The future XENON-1T (2017) will exclude large parameter space of this region, but a small fraction can still survived when dark matter mass is very close to half the Z mass or Higgs mass. It should be noted the some points within the 2σ range of PLANCK still survived the LUX search. But they are possibly covered by future dark matter Direct search XENON-1T (2017).

So, in the following, we concentrate on the points which are still survived under limits from the dark matter experiments. Although in this region, a correct relic abundance could be derived by elaborately tuning the neutralino mass, we just take the dark matter relic abundance as an upper limit here.

III. DIRECT SEARCH LIMITS ON THE PARAMETER SPACE

At LHC, the ATLAS and CMS collaborations have separately preform the $3l$ searches [20, 21]. They aims at the $\chi_2^0 \chi_1^\pm$ pair production following by decays $\chi_2^0 \rightarrow \chi_1^0 + Z$, $\chi_1^\pm \rightarrow \chi_1^0 + W^\pm$ (the W and Z can be virtual), and then the W/Z decays producing 3 leptons in the final state. In this paper, we use the ATLAS experiment result to constrain our parameter

space.

The ATLAS experiment[30] defines six signal regions aiming at Z -depleted region and Z -enriched region. Table II shows the selection requirements of these six signal regions. We can see that SRnoZ(a,b,c) concentrate on the Z -depleted case where the invariant mass of the SFOS lepton pair departs the Z -boson mass. Conversely, in the other three regions, a Z boson is required in the mediate state.

Through the analysis, the experiments give an exclusion region on the $\chi_2^0 - \chi_1^0$ plane and the exclusion limit can reach 320 GeV¹. It should be noted that in the experiments a wino like NLSP and bino LSP are assumed and the decay branching ratio of $\chi_2^0 \rightarrow \chi_1^0 + Z$ and $\chi_1^\pm \rightarrow \chi_1^0 + W^\pm$ are set to be 100%.

In the higgsino NLSP case, not only the χ_2^0 , but also the χ_3^0 contributes to the signals. Even so, the total cross section is still about half of the one in the wino case. So we should carefully implement the $3l$ experiments on our parameter space; in the present work, we use the Monte Carlo simulation. **MadGraph5** [31] are adopted to generate events, the parton shower is carried out by **PYTHIA** [32], and **CheckMATE1.1.4** [33] are used to simulate the $3l$ experiments events. Finally, we combine the simulation results from the six signal regions and derive the final exclusion limit. At the beginning, we checked the reliability of our simulation with the benchmark points provided by ATLAS paper; we found them well consistent.

Figure 2 shows our limit assuming a 100% branching ratio of $\chi_2^0 \rightarrow \chi_1^0 + Z$ and $\chi_3^0 \rightarrow \chi_1^0 + Z$. We can see the limit can reach utmost 250 GeV when the LSP is near to 0 GeV, comparing to the limit 320 GeV in the wino case. It also tells when the LSP becomes heavy, the limit reduces rapidly. This figure is also consistent with similar figures provided by other authors[18]. We should note that there is a part where the limit is not effective. It locates around $M_{\chi_2^0} \sim 140 - 160$ GeV and $M_{\chi_1^0} \sim 40 - 60$ GeV. It can be explained as follows. When the splitting of χ_2^0 and χ_1^0 is just larger than the Z mass, this kinematics is very similar to the one of WZ background and thus its backgrounds are relatively large. Then this region has a small probing efficiency.

To impose the $3l$ constraint on our samples, it should also survey the decay branching

¹ We note that in the latest ATLAS $3l$ results this limit reaches 345 GeV. We carefully check the difference between the old one and the latest one, and find that the cut efficiency is not improved significantly and the latest result is also hard to implement because twenty signal regions are defined.

TABLE I: The selection requirements for the six signal regions.

Selection	SRnoZa	SRnoZb	SRnoZc	SRZa	SRZb	SRZc
m_{SFOS} [GeV]	< 60	60-81.2	<81.2 or > 101.2	81.2-101.2	81.2-101.2	81.2-101.2
E_T^{miss} [GeV]	>50	>75	>75	75-120	75-120	>120
m_T [GeV]	—	—	>110	<110	>110	>110
$p_T^{3rd\ l}$ [GeV]	>10	>10	>30	>10	>10	>10
SR veto	SRnoZc	SRnoZc	—	—	—	—

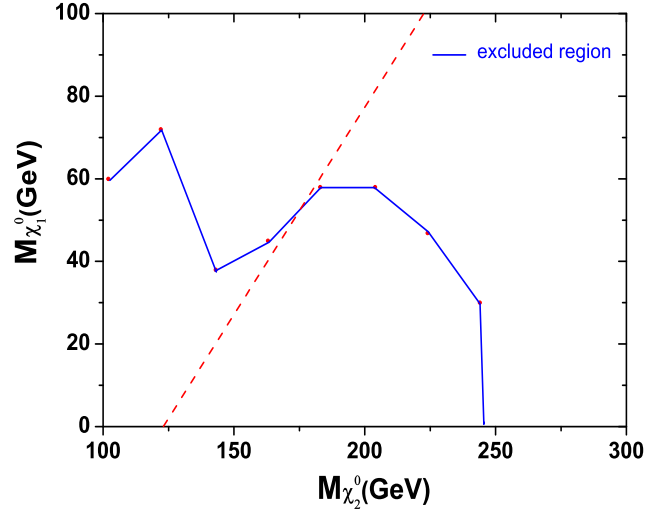


FIG. 2: The $3l$ exclusion limit on the $\chi_2^0 - \chi_1^0$ plane with higgsino being the NLSP and a 100% branching ratio of $\chi_{2,3}^0 \rightarrow \chi_1^0 + Z$ is assumed. The red dashed line is the dividing line $m_{\chi_2^0} = m_{\chi_1^0} + m_h$. On the right part of this line, the decay channel of $\chi_2^0 \rightarrow \chi_1^0 h$ opens.

ratio of $\chi_{2,3}^0$. Fig. 3 presents the decays of $\chi_{2,3}^0$ ($\chi_{2,3}^0 \rightarrow \chi_1^0 Z$ including off-shell Z). When $\chi_1^0 h$ channel does not open, the $\chi_{2,3}^0 \rightarrow \chi_1^0 Z$ dominates. Otherwise, we can see two distinct regions for the decays of $\chi_{2,3}^0$, the h -enriched region and the h -depressed region. In the h -enriched region, the branching ratio of $\chi_{2,3}^0 \rightarrow \chi_1^0 h$ can reach as much as 75%, whereas in the h -depressed region, this branching ratio would be less than 25%.

Note that $\chi_2^0 \rightarrow \chi_1^0 h$ and $\chi_3^0 \rightarrow \chi_1^0 h$ can not be enriched at the same time, which can be inferred from the third panel of Fig. 3. The reason is illustrated clearly in paper[19, 34]. It also should point out that the $3l$ probing ability is relevant to the $Br(\chi_2^0 \rightarrow \chi_1^0 Z) + Br(\chi_3^0 \rightarrow$

$\chi_1^0 Z$).

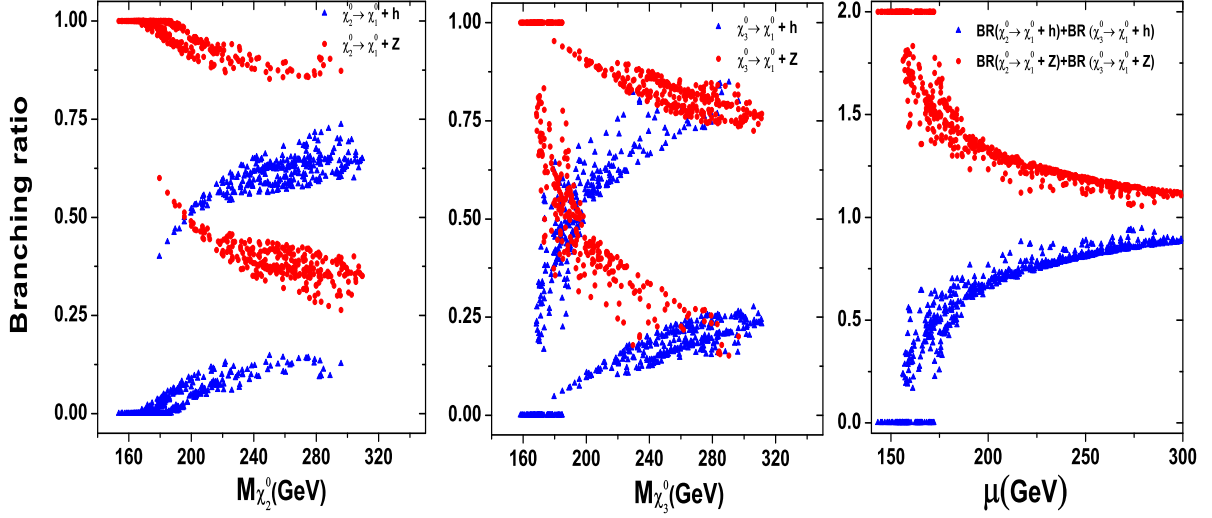


FIG. 3: The decay branching ratio of the neutralinos.

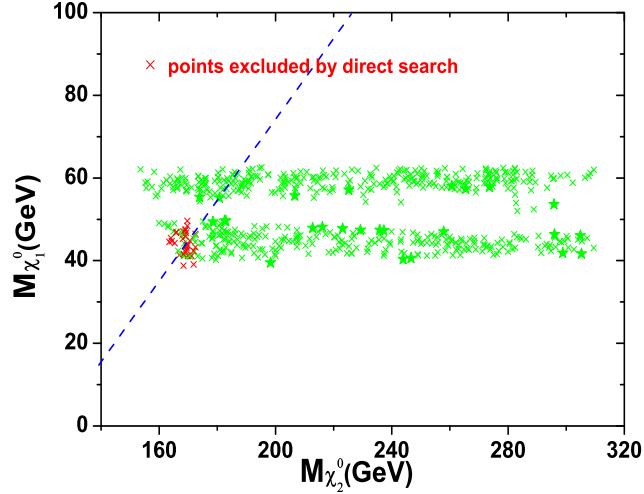


FIG. 4: The $3l$ exclusion results considering branching ratio effect. The blue dashed line is the dividing line $m_{\chi_2^0} = m_{\chi_1^0} + m_h$. On the right part of this line, the decay channel of $\chi_2^0 \rightarrow \chi_1^0 h$ opens. The pentagams on the plot satisfying the 2σ range of PLANCK.

Figure 4 presents the limit at 8 TeV LHC on the parameter space considering the branching ratio effect. It is found that only a very tiny region can be excluded in this scenario

and most regions survived. The blue line represents the threshold $\chi_2^0 \rightarrow \chi_1^0 h$. Only the points near the bottom of the line have been excluded. The points which survives lying the left part of the line escape from the experimental limits largely due to a suppression on the kinematics cut. And the reason for the points surviving on the right part of the line is the $\chi_2^0 \rightarrow \chi_1^0 h$ channel opens and the reduce of $\chi_{2,3}^0 \chi_1^\pm$ production rate. Note that even the $\chi_2^0 \rightarrow \chi_1^0 h$ channel opens, there are still points excluded. The reason is that when the $\chi_2^0 \rightarrow \chi_1^0 h$ is just open, the branching ratio of $\chi_{2,3}^0 \rightarrow \chi_1^0 h$ is still very small, which can be seen from the right panel of Fig. 3. We note the points satisfying the relic density are still relatively safe.

In addition, the mass of χ_2^0 in our surviving samples is larger than 150 GeV. It is largely due to the Z invisible decay and Higgs invisible decay limit because a fraction of Higgsino component of dark matter would sizably affect the decays of Z boson and Higgs boson.

IV. PROBING PROSPECTS IN FUTURE LHC

The discovery potential at 14 TeV LHC are discussed in this section. Although the $\chi_{2,3}^0 \chi_1^\pm$ production rate will increase at 14 TeV LHC, the background will enlarge too. We must simulate the backgrounds as well as the signals. The irreducible background includes diboson, triboson and $t\bar{t}W/Z$ production, among which the diboson production highly dominates. The reducible background includes single and pair production of top quarks, WW and single W or Z boson processes produced in association with jets or photons, among which the $t\bar{t}$ production highly dominates. In our paper we only simulate the mainly backgrounds: the diboson backgrounds and the $t\bar{t}$ backgrounds. We use **MadGraph** simulate our backgrounds and scale the cross sections to the next leading order [35]. To make our backgrounds more accurate, we first simulate the backgrounds at 8TeV. After comparing our simulated backgrounds and the backgrounds derived from experimental results, we get the scale factors in each signal region. Then we multiply the corresponding scale factors on our simulated 14TeV backgrounds and then we take these scaled 14TeV backgrounds as our backgrounds. Although at 14 TeV LHC the scaled factors might be changed a little, it still offset some deviation between our simulations and the experimental background estimation.

In Table 1 lists the number of background events at 14 TeV LHC 300 fb⁻¹. In the Z -enriched region, WZ production dominates the background, whereas in the Z -depleted

region, the $t\bar{t}$ has a comparative contribution.

TABLE II: The number of background events at 14 TeV LHC 300 fb⁻¹.

Background	SRnoZa	SRnoZb	SRnoZc	SRZa	SRZb	SRZc
ZZ	410	59	10	280	39	12
ZW^\pm	1391	595	71	6850	661	189
$t\bar{t}$	1715	401	62	272	178	19
Total	3516	1055	143	7402	878	220

For the signal, the cross section are calculated using **Prospino2.1** [36]. We implement the same cuts on the signal and backgrounds. The following formulas are adopted to calculate the significance

$$\text{Significance} = \frac{S}{\sqrt{B + (0.1B)^2}} \quad (3)$$

where S is the number of signal events and B is the total number of background events. We also considered 10% sys. error in the estimation.

We present the final results in Fig. 5. It shows that the region with $40 \text{ GeV} \lesssim m_{\tilde{\chi}_1^\pm} \lesssim 60 \text{ GeV}$ and $160 \text{ GeV} \lesssim m_{\tilde{\chi}_{2,3}^0} \lesssim 300 \text{ GeV}$ can be covered at 3σ level. Some parameter space can reach the 5σ discovery level. We note here the points satisfying the 2σ range of PLANCK would be easily covered at 2σ level. A tiny part of the parameter space is under 2σ because it locates at the region where the kinematics similar to the WZ background. However, if the luminosity increases, this region would be more squeezed.

Finally, we stress that our analysis is performed in the framework of MSSM. In some extensions of the MSSM, such as the next-to-minimal supersymmetric standard model (NMSSM) which seems to be more favored by the LHC Higgs data [37], the neutralino LSP may have a significant singlino component and thus can be very light [38]. Then the $\tilde{\chi}_1^\pm \tilde{\chi}_{2,3}^0$ production may have different signatures.

V. CONCLUSION

Motivated by the naturalness, we study a simplified MSSM scenario where only the bino-like LSP and higgsino-like NLSP are light. We first scan the parameter space of this scenario,

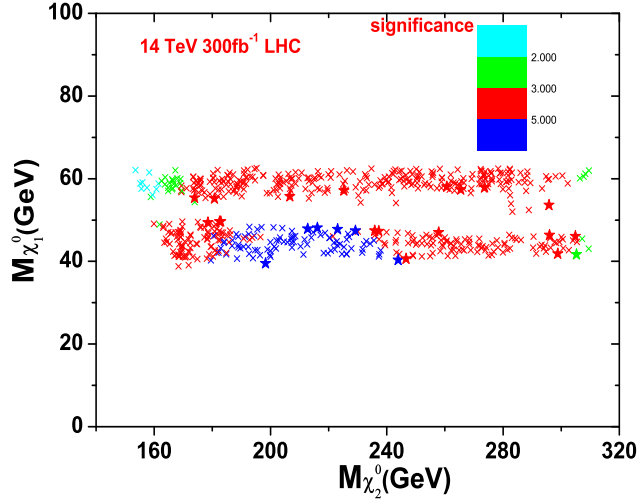


FIG. 5: The discovery potential at 14 TeV LHC with 300 fb⁻¹. The pentagrams on the plot satisfying the 2 σ range of PLANCK.

considering the constraints from the Higgs mass, flavor physics, electroweak precision measurements and dark matter experiments. Then in the allowed parameter space, we perform a Monte Carlo simulation for the $\tilde{\chi}_1^\pm \tilde{\chi}_{2,3}^0$ production followed by $\tilde{\chi}_1^\pm \rightarrow W^\pm \tilde{\chi}_1^0$ and $\tilde{\chi}_{2,3}^0 \rightarrow Z \tilde{\chi}_1^0$. By examining the presently available trilepton bounds on the wino-like chargino/neutralino, we find that only a narrow region $40 \text{ GeV} \lesssim m_{\tilde{\chi}_1^0} \lesssim 50 \text{ GeV}$ and $160 \text{ GeV} \lesssim m_{\tilde{\chi}_{2,3}^0} \lesssim 170 \text{ GeV}$ on the plane of $m_{\tilde{\chi}_1^0} - m_{\tilde{\chi}_{2,3}^0}$ can be excluded. Finally, we explore the potential of trilepton signature in probing such a scenario at 14 TeV LHC and find that the region with $40 \text{ GeV} \lesssim m_{\tilde{\chi}_1^0} \lesssim 60 \text{ GeV}$ and $160 \text{ GeV} \lesssim m_{\tilde{\chi}_{2,3}^0} \lesssim 300 \text{ GeV}$ can be covered at 3 σ level with luminosity $\mathcal{L} = 300 \text{ fb}^{-1}$.

Acknowledgement

I would like to thank Junjie Cao, Jie Ren, Lei Wu, Jin Min Yang and Yang Zhang for helpful discussions and valuable comments on the manuscript. I acknowledge the Korea Ministry of Education, Science and Technology (MEST) for the support of the Young Scientist Training Program at the Asia Pacific Center for Theoretical Physics (APCTP).

-
- [1] G. Aad *et al.* [ATLAS Collaboration], Phys. Lett. B **716**, 1 (2012); S. Chatrchyan *et al.* [CMS Collaboration], Phys. Lett. B **716**, 30 (2012).
 - [2] J. R. Ellis, K. Enqvist, D. V. Nanopoulos, and F. Zwirner, Mod. Phys. Lett. A **1** (1986) 57; R. Barbieri and G. Giudice, Nucl. Phys. B **306** (1988) 63;
 - [3] C. Brust, A. Katz, S. Lawrence and R. Sundrum, JHEP **1203**, 103 (2012).
 - [4] M. Papucci, J. T. Ruderman and A. Weiler, JHEP **1209**, 035 (2012).
 - [5] L. J. Hall, D. Pinner and J. T. Ruderman, JHEP **1204**, 131 (2012);
 - [6] M. Dine, A. Kagan and S. Samuel, Phys. Lett. B **243**, 250 (1990). A. Cohen, D. B. Kaplan and A. Nelson, Phys. Lett. B **388**, 588 (1996); H. Baer *et al.*, JHEP **1010**, 018 (2010); D. Feldman, G. Kane, E. Kuflik and R. Lu, Phys. Lett. B **704**, 56 (2011);
 - [7] G. W. Anderson, D. J. Castano and A. Riotto, Phys. Rev. D **55**, 2950 (1997); K. L. Chan, U. Chattopadhyay and P. Nath, Phys. Rev. D **58**, 096004 (1998); J. L. Feng, K. T. Matchev and T. Moroi, Phys. Rev. D **61**, 075005 (2000); J. Hisano, K. Kurosawa and Y. Nomura, Nucl. Phys. B **584**, 3 (2000); R. Kitano and Y. Nomura, Phys. Rev. D **73**, 095004 (2006); M. Asano *et al.*, JHEP **1012**, 019 (2010); S. Akula *et al.*, Phys. Lett. B **709**, 192 (2012); G. Bhattacharyya and T. S. Ray, JHEP **1205**, 022 (2012); S. Krippendorff *et al.*, Phys. Lett. B **712**, 87 (2012); B. C. Allanach and B. Gripaios, JHEP **1205**, 062 (2012); H. Baer *et al.*, JHEP **1205**, 109 (2012); J. L. Feng and D. Sanford, Phys. Rev. D **86**, 055015 (2012); L. Randall and M. Reece, arXiv:1206.6540 [hep-ph]; C. Wymant, Phys. Rev. D **86**, 115023 (2012); H. Baer *et al.*, Phys. Rev. Lett. **109** (2012) 161802; Phys. Rev. D **87**, 115028 (2013); P. Lodone, Int. J. Mod. Phys. A **27** (2012) 1230010; H. M. Lee, V. Sanz, and M. Trott, JHEP **1205** (2012) 139; E. Arganda, J. L. Diaz-Cruz and A. Szykman, Phys. Lett. B **722**, 100 (2013); E. Hardy, arXiv:1306.1534 [hep-ph]; M. Blanke, *et al.*, JHEP **1306** (2013) 022; B. Bhattacharjee, *et al.*, arXiv:1301.2336 [hep-ph]; C. Han, F. Wang and J. M. Yang, arXiv:1304.5724 [hep-ph]; G. Altarelli, arXiv:1308.0545 [hep-ph]; Z. Kang, J. Li and T. Li, JHEP **1211** (2012) 024.
 - [8] C. Han, *et al.*, JHEP **1310** (2013) 216 [arXiv:1308.5307 [hep-ph]]; J. Cao, *et al.*, JHEP **1211** (2012) 039 [arXiv:1206.3865 [hep-ph]].
 - [9] R. Boughezal and M. Schulze, arXiv:1212.0898 [hep-ph]; M. L. Graesser and J. Shelton, arXiv:1212.4495 [hep-ph]; Z.-H. Yu *et al.*, Phys. Rev. D **87**, 055007 (2013); G. Belanger *et*

- et al.*, JHEP **1305**, 167 (2013); R. Franceschini and R. Torre, Eur. Phys. J. C **73**, 2422 (2013); D. Ghosh and D. Sengupta, Eur. Phys. J. C **73**, 2342 (2013); X.-J. Bi, Q.-S. Yan and P.-F. Yin, Phys. Rev. D **87**, 035007 (2013); C.-Y. Chen *et al.*, JHEP **1211**, 124 (2012); E. L. Berger *et al.*, Phys. Rev. Lett. **109**, 152004 (2012); P. Agrawal and C. Frugiuele, arXiv:1304.3068 [hep-ph]; J. Guo *et al.*, arXiv:1308.3075 [hep-ph].
- [10] Z. Han *et al.*, JHEP **1208**, 083 (2012).
- [11] M. Drees, M. Hanussek and J. S. Kim, arXiv:1201.5714 [hep-ph]; M. Drees, M. Hanussek and J. S. Kim, arXiv:1304.7559 [hep-ph]; A. Delgado *et al.*, Eur. Phys. J. C **73**, 2370 (2013).
- [12] G. Brooijmans *et al.*, arXiv:1405.1617 [hep-ph]; C. Han, *et al.*, JHEP **1402** (2014) 049 [arXiv:1310.4274 [hep-ph]]; P. Schwaller and J. Zurita, JHEP **1403** (2014) 060; G. F. Giudice *et al.*, Phys. Rev. D **81**, 115011 (2010); H. Baer, A. Mustafayev and X. Tata, Phys. Rev. D **89** (2014) 055007.
- [13] A. Anandakrishnan, L. M. Carpenter and S. Raby, Phys. Rev. D **90**, 055004 (2014).
- [14] T. Liu, L. Wang and J. M. Yang, Phys. Lett. B **726**, 228 (2013).
- [15] S. Gori, S. Jung and L. T. Wang, JHEP **1310** (2013) 191; Z. Han, *et al.*, Phys. Rev. D **89** (2014) 075007.
- [16] J. Bramante, *et al.*, arXiv:1408.6530 [hep-ph].
- [17] C. Han, *et al.*, arXiv:1409.4533 [hep-ph].
- [18] See recent examples after 125 GeV Higgs, J. S. Kim and T. S. Ray, arXiv:1405.3700 [hep-ph]; G. Barenboim, *et al.*, Phys. Rev. D **90** (2014) 035020 [arXiv:1407.1218 [hep-ph]]; T. Han, S. Padhi and S. Su, Phys. Rev. D **88** (2013) 115010 [arXiv:1309.5966 [hep-ph]]; T. Han, Z. Liu and S. Su, JHEP **1408** (2014) 093 [arXiv:1406.1181 [hep-ph]]; M. Berggren, *et al.*, arXiv:1309.7342 [hep-ph]; U. Ellwanger and A. M. Teixeira, arXiv:1406.7221 [hep-ph]; U. Ellwanger, JHEP **1311**, 108 (2013) [arXiv:1309.1665 [hep-ph]]; K. Hikasa *et al.*, JHEP **1407**, 065 (2014) [arXiv:1403.5731 [hep-ph]]; C. Cheung *et al.*, JHEP **1305**, 100 (2013); T. A. W. Martin and D. Morrissey, arXiv:1409.6322 [hep-ph]; M. Chakraborti *et al.*, JHEP **1407** (2014) 019; D. Ghosh, M. Guchait and D. Sengupta, Eur. Phys. J. C **72** (2012) 2141; P. Byakti and D. Ghosh, Phys. Rev. D **86** (2012) 095027.
- [19] T. Han, S. Padhi and S. Su, Phys. Rev. D **88** (2013) 115010 [arXiv:1309.5966 [hep-ph]].
- [20] G. Aad *et al.* [ATLAS Collaboration], JHEP **1404**, 169 (2014) [arXiv:1402.7029 [hep-ex]].
- [21] V. Khachatryan *et al.* [CMS Collaboration], arXiv:1405.7570 [hep-ex].

- [22] M. Frank *et al.*, JHEP **0702**, 047 (2007); G. Degrandi *et al.*, Eur. Phys. J. C **28**, 133 (2003); S. Heinemeyer, W. Hollik and G. Weiglein, Comput. Phys. Commun. **124**, 76 (2000); Eur. Phys. J. C **9**, 343 (1999).
- [23] P. Bechtle *et al.*, Comput. Phys. Commun. **182**, 2605 (2011); Comput. Phys. Commun. **181**, 138 (2010).
- [24] F. Mahmoudi, Comput. Phys. Commun. **180**, 1579 (2009); Comput. Phys. Commun. **178**, 745 (2008).
- [25] J. Cao and J. M. Yang, JHEP **0812**, 006 (2008).
- [26] P. A. R. Ade *et al.* [Planck Collaboration], arXiv:1303.5076 [astro-ph.CO].
- [27] G. Belanger *et al.*, Comput. Phys. Commun. **182**, 842 (2011).
- [28] N. Arkani-Hamed, A. Delgado and G. F. Giudice, Nucl. Phys. B **741** (2006) 108; C. Cheung, *et al.*, JHEP **1305** (2013) 100; T. Han, Z. Liu and A. Natarajan, JHEP **1311** (2013) 008; F. Wang, W. Wang and J. M. Yang, arXiv:1310.1750 [hep-ph]; P. Huang and C. E. M. Wagner, Phys. Rev. D **90** (2014) 015018; J. Edsjo and P. Gondolo, Phys. Rev. D **56** (1997) 1879 [hep-ph/9704361]; K. Griest and D. Seckel, Phys. Rev. D **43** (1991) 3191.
- [29] D. S. Akerib *et al.* [LUX Collaboration], Phys. Rev. Lett. **112** (2014) 091303 [arXiv:1310.8214 [astro-ph.CO]].
- [30] ATLAS Collaboration, ATLAS-CONF-2013-035
- [31] J. Alwall *et al.*, JHEP **1106**, 128 (2011).
- [32] T. Sjostrand, S. Mrenna and P. Z. Skands, JHEP **0605**, 026 (2006).
- [33] M. Drees, *et al.*, arXiv:1312.2591 [hep-ph].
- [34] S. Jung, JHEP **1406** (2014) 111 [arXiv:1404.2691 [hep-ph]].
- [35] J. M. Campbell, R. K. Ellis and C. Williams, JHEP **1107** (2011) 018 [arXiv:1105.0020 [hep-ph]]; R. Bonciani, *et al.*, Nucl. Phys. B **529** (1998) 424 [Erratum-ibid. B **803** (2008) 234] [hep-ph/9801375].
- [36] W. Beenakker *et al.*, Nucl. Phys. B **515**, 3 (1998);
- [37] J. Cao *et al.*, JHEP **1203**, 086 (2012) [arXiv:1202.5821 [hep-ph]]; JHEP **1210**, 079 (2012) [arXiv:1207.3698 [hep-ph]].
- [38] J. Cao *et al.*, JHEP **1405**, 056 (2014) [arXiv:1311.0678 [hep-ph]].